Available online at www.sciencedirect.com

ScienceDirect

St. Petersburg Polytechnical University Journal: Physics and Mathematics 1 (2015) 37–41

www.elsevier.com/locate/spjpm

Microfabricated cells for chip-scale atomic clock based on coherent population trapping: Fabrication and investigation

S.V. Ermak [a,*], V.V. Semenov [a], E.N. Piatyshev [a], A.N. Kazakin [a], I.M. Komarevtsev [a], E.N. Velichko [a], V.V. Davydov [a], M.V. Petrenko [b]

[a] *St. Petersburg Polytechnic University, 29 Politekhnicheskaya St., Petersburg 195251, Russian Federation*
[b] *Ioffe Physical-Technical Institute, 26 Politekhnicheskaya St., Petersburg, 194021, Russian Federation*

Available online 11 March 2015

Abstract

A universal method for fabrication of miniature cells for frequency standards and quantum magnetometers containing ^{87}Rb atoms in the atmosphere of inert gas neon based on integrated technologies is considered. The results of experimental studies of coherent population trapping signals observed for a series of cells which provided recovery of vapors of an alkali metal from the rubidium dichromate salt with the help of laser radiation are presented. The coherent population trapping signals with a typical linewidth of 2–3 kHz and a signal-to-noise ratio of 1500 in the 1-Hz bandwidth were observed, which allows one to provide a relative frequency stability of atomic clock of 10^{-11} at 100 s.

Keywords: Laser spectroscopy; Coherent population trapping; MEMS technology; Microfabricated cell; Alkali atom; Quantum frequency standard.

1. Introduction

A growing interest in small-size telecommunications systems having various applications has brought significant advances in development of miniature quantum devices to which chip-scale atomic clocks (CSACs) and chip-scale quantum magnetometers (CSQMs) belong. Miniature CSACs are used to synchronize the operation of electronic devices and to set a precise time in portable applications where a small size, a low power consumption, a good long-term stability, and resistance to considerable mechanical perturbations are important [1]. Small-size CSQMs in the form of compact matrix-type sensors find application in a variety of biomagnetic studies [2]. Basic elements of miniature CSACs and CSQMs are a laser source (single-mode vertical-cavity surface-emitting laser VCSEL) and a cell that contains alkali metal atoms (typically ^{87}Rb, ^{85}Rb, ^{133}Cs) in a buffer gas atmosphere. The cell quality strongly depends on the amount of alkali metal, the buffer gas pressure and composition, and the presence of impurities in the cell and directly affects the stability and reproducibility of the CSAC and CSQM characteristics. The

* Corresponding author.
E-mail addresses: serge_ermak@mail.ru (S.V. Ermak), vladimir_semenov@mail.ru (V.V. Semenov), pen@mems.ru (E.N. Piatyshev), keha@newmail.ru (A.N. Kazakin), vanec@aport.ru (I.M. Komarevtsev), velichko-spbstu@yandex.ru (E.N. Velichko), davydov_vadim66@mail.ru (V.V. Davydov), m.petrenko@mail.ioffe.ru (M.V. Petrenko).

http://dx.doi.org/10.1016/j.spjpm.2015.03.003

(Peer review under responsibility of St. Petersburg Polytechnic University).

most appropriate technology that can ensure a high quality of cells for such devices is the microelectromechanical systems (MEMS) manufacturing technology. It combines the advantages offered by the techniques of microelectronic component fabrication and manufacturing and assembling miniature mechanical systems [3]. The great importance for miniature CSACs and CSQMs design have the method of a resonance signal inducing for comparison an atom transition frequency with the frequency of the reference oscillator. Classical analogs of precision quantum devices use the method of double radio–optical resonance (DROR) [4,5]. The use of the microwave volume resonators hinders for the device miniaturization. In this case, the effect of coherent population trapping (CPT) is extremely attractive because it does not require the use of microwave resonators and ensures the formation of a sufficiently reliable resonance signal under the conditions of interaction between the working substance atoms and the optical field of the pump laser [6,7].

2. Method for cells manufacturing

For the studies, cells with a universal construction (Fig. 1) were fabricated. The microfabricated cells were designed so that they could be included into the optical path in two ways: in the transmission mode for the cells with a thickness more than 1 mm (Fig. 2a) [8,9] or with a double reflection of the pump beam from inner walls of the cells with a submillimeter thickness

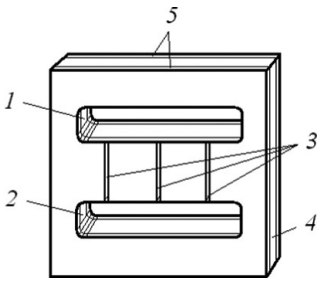

Fig. 1. Microfabricated cell: *1*, *2* – working and additional cavity, respectively, *3* – connecting channels, *4*, *5* – silicon and glass plates, respectively.

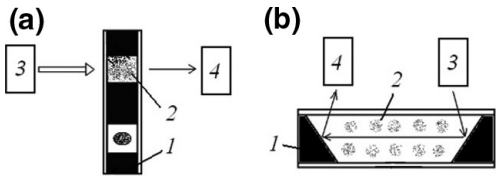

Fig. 2. Cell (*1*) incorporation into the optical path: pump beam is transmitted through the cavity (a), pump beam passes along the channel with reflections (b), *2* – working cavity, *3* – laser, *4* – photoreceiver.

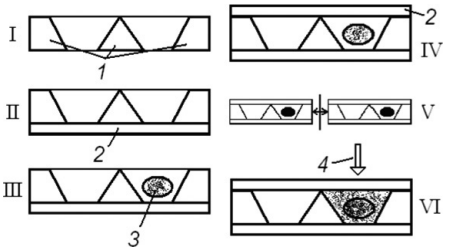

Fig. 3. Stages of cell fabrication: I – alkaline etching of silicon; II, IV – bonding of the first and second glass plates; III – placing titanium mini-tablet with rubidium dichromate; V – separation into chips; VI – laser activation; *1* – silicon, *2* – glass, *3* – rubidium dichromate, *4* – laser beam.

(Fig. 2b) [1]. The additional cavity 2 (see Fig. 1) was necessitated by the use of the method of recovery of an alkali metal from the rubidium dichromate salt including interaction of a material with an activating laser radiation [10]. Channels 3 (see Fig. 1) provided, due to a small cross-section, a transfer of rubidium atoms into the working cavity without byproducts formed during recovery of alkali vapors.

Fig. 3 shows schematically a simultaneous fabrication of 97 cells. At the first stage (I) of the technological process, cavities were etched by a deep alkaline etching through the entire thickness of the KEF-20 silicon wafer with the (100) orientation. The etching was carried out in a 30% aqueous solution of potassium hydroxide during 8 h at 80 °C. At the second stage (II), a flat glass plate (LK5 glass) was attached to the bottom side of the silicon wafer by using anodic bonding in air at 450 °C under a voltage of 800 V for 30 min. At the third stage (III), a titanium mini-tablet containing a few percent of rubidium dichromate about 200 μm in diameter was placed into each of the 97 cells by using a special mask. At the fourth stage (IV), the second glass plate was attached to the upper side of the silicon wafer by anodic bonding. Bonding was performed in a neon atmosphere (under a pressure of 200 mmHg) during 2 h at 400 °C, under a voltage of 350 V. Prior to bonding, all elements were outgassed under vacuum (under pressure of 10^{-4} mmHg) at 450 °C for an hour. At the fifth stage (V), the three-layer structure (glass–silicon–glass) was separated into chips by a diamond cutting disk. At the sixth stage (VI), each tablet was activated by an IR laser.

3. Investigation of cell characteristics

To study experimentally the small-size cells prepared by the procedure described above, the setup presented schematically in Fig. 4 was used. A laser beam (L) was

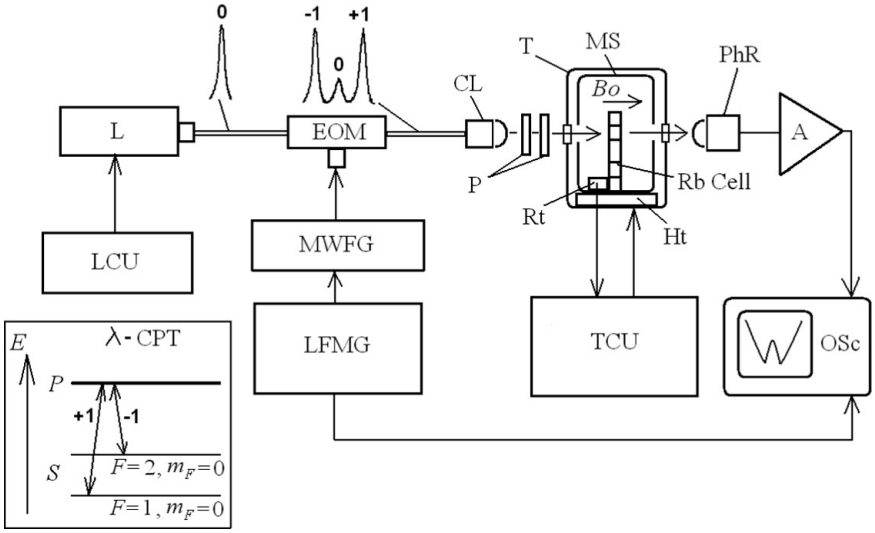

Fig. 4. Experimental setup: L – laser, EOM – electrooptical modulator, MWFG – microwave generator, CL – collimator, P – polaroids, Rb Cell – cell with rubidium, PhR – photoreceiver, A – amplifier, OSc – oscilloscope, T – thermostat, TCU – thermostat control unit, Ht – heater, Rt – thermistor, MS – magnetic shield, LCU – laser control unit, LFMG – low-frequency modulation generator, λ-CPT – a simplified structure of energy levels in rubidium in the case the CPT signal is produced according to the λ-scheme.

fed to an electrooptical phase modulator (EOM) modulated by a sinewave signal from a microwave generator (MWFG). At the EOM output, the first order spectral -1 and $+1$ components separated by twice the frequency of the modulating microwave signal appeared. The carrier component "0" was suppressed by 70% as compared with its intensity at the EOM input. Then the light passed through a collimator (CL) and polaroids P (λ/2 and λ/4), was partially absorbed in the cell (Rb Cell) and was detected by a photoreceiver (PhR). After that the signal amplified by an amplifier (A) was fed to the oscilloscope (OSc) input.

The cell temperature was stabilized by a thermostat (T) that included a heating element (Ht) and a thermistor (Rt) that provided measurements of the cell temperature. The thermostat was controlled by a control unit (TCU). A magnetic shield (MS) screened the cell from external magnetic fields, the internal magnetic field B_0 was produced by a built-in coil. A low-frequency modulation generator (LFMG) provided the modulation of the resonance conditions for observation of CPT signals. A laser control unit (LCU) was used to stabilize laser current and temperature and to weakly modulate the laser current in order to observe the absorption spectra of ^{87}Rb atoms.

In the experiment, the radiation absorption signal was detected by scanning its frequency in the region of the D_2 line of absorption of ^{87}Rb atoms. The absorption cavity was placed in the optical path according to the scheme shown in Fig. 2a (microwave EOM

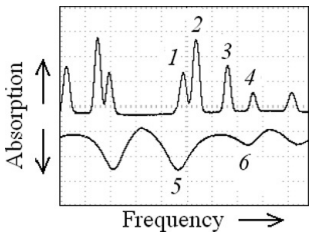

Fig. 5. Oscillogram of absorption spectra for two cells: reference cell (top) and working cell (bottom). Peak identification: *1*, *5* – LF-components of ^{87}Rb, *4*, *6* – HF-components of ^{87}Rb; *2*, *3* – LF- and HF-components of ^{85}Rb.

modulation was turned off). The pump source was a semiconductor laser with an external resonator operating in a continuous single-frequency mode and having a spectral linewidth of 500 kHz. The pump power was 50 μW at a beam aperture of 2 mm^2. The radiation receiver was a photodiode with a reduced dark current level [11,12]. To increase the vapor density of the working substance, the cell was heated to a temperature of 100 °C. Fig. 5 shows the absorption spectra of laser radiation for two cells: a reference cell (not shown in Fig. 4) containing a mixture of ^{87}Rb and ^{85}Rb isotopes (top) and microfabricated cell (bottom). A considerable broadening of absorption lines of ^{87}Rb atoms in the microfabricated cell (more than 1 GHz) (see Fig. 5, lines 5 and 6) was due to a high temperature and the presence of the buffer neon gas in the cell having a relatively high pressure (100 mmHg).

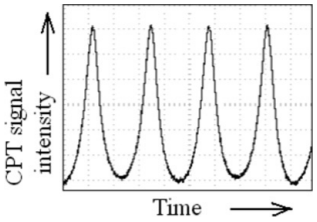

Fig. 6. Oscilloscope traces of CPT signal: resonance line is shown.

The 20–50% level of the resonance absorption of the incident radiation indicated that the amount of ^{87}Rb atoms in the cavity was high enough to observe a CPT signal.

To form the CPT signal, a sinewave modulation signal with the frequency equal to half the resonant frequency of the magnetically independent microwave (0–0) transition (6.834682 GHz) from the microwave generator with a power of 10 dBm was applied to the electrooptical modulator (see Fig. 4). The spectrum of the phase-modulated pump radiation contained two coherent components with the spectral interval equal to the frequency of the magnetically independent (0–0) transition of working substance atoms. The CPT signals (Fig. 6) had a typical linewidth of 2–3 kHz and a signal/noise ratio of 1500 in the 1 Hz bandwidth were observed. The experimental data allowed us to estimate the relative short-term instability of CPT-based atomic clocks during the measuring time t (in seconds) as [13]

$$\sigma = \left[\left(\frac{S}{N}\right)_{1\,\mathrm{Hz}} \times Q\right]^{-1} t^{-1/2}, \qquad (1)$$

where $(S/N)_{1\ \mathrm{Hz}}$ is the signal-to-noise ratio in the 1-Hz band; and Q is the quality factor of the resonance equal to the ratio between the frequency of transition and its width.

By substituting the resonance line parameters into expression (1), we obtain the estimate of the relative frequency instability $\sigma = 1.4 \times 10^{-10}\, t^{-1/2}$ during the measuring time t (s), which predicts the frequency instability of 10^{-11} at 100 s, which is satisfactory for miniature CSACs [1,14].

4. Conclusions

The results obtained in studies of parameters of resonance CPT signals from microfabricated cell with a working cavity volume of 1.2 mm^3 manufactured using the MEMS technique suggest that this technique is efficient for the development of CSACs and CSQMs with laser pumping and relative frequency stability (CSACs) of $1.4 \times 10^{-10}\, t^{-1/2}$. To use other lasers (e.g. with broadened spectral line and relatively unstable VCSELs), the cell fabrication technique should be modified. This refers to the optimization of cell filling, temperature and pumping regimes, and also a need for additional magnetic shielding (for CSACs) with the aim of reducing the orientation and light shifts and maximizing the long-term frequency stability of CSACs and CSQMs [15–18]. For example, a dosed filling of the cells with an alkali metal can allow one to avoid the metal recovery phase and to improve the cell quality. The presence of impurities will be excluded in this case, which will enable reduction in the cell sizes, while retaining a satisfactory long-term stability of resonance signals.

References

[1] R. Lutwak, Principles of Atomic Clocks, Tutorial of EFTF-IFCS, 2011.
[2] G. Bison, R. Wynands, A. Weis, A laser-pumped magnetometer for the mapping of human cardio-magnetic fields, Appl. Phys. B 76 (2003) 325.
[3] E.N. Pyatyshev, M.S. Lurie, I.V. Popova, A.N. Kazakin, Spetsifika tekhnologii mikromekhanicheskikh ustrojstv (The peculiarities of the technology of micromechanical devices), J. Nano Microsyst. Tech. 6 (2001) 32–34.
[4] W. Happer, Optical pumping, Rev. Mod. Phys. 44 (1972) 169–249.
[5] M. Bloch, I. Pascaru, C. Stone, T. Mcclelland, Subminiature rubidium frequency standard for commercial applications, in: Proceedings of the 47th IEEE IFCS, IEEE, 1993, pp. 164–177.
[6] E. Arimondo, G. Orriols, Non-absorbing atomic coherences by coherent 2-photon transitions in a 3-level optical pumping, Lett. Nuovo Cimento 17 (1976) 333–338.
[7] J. Vanier, Atomic clocks based on coherent population trapping: a review, Appl. Phys. B Lasers Opt. 81 (2005) 421–442.
[8] S. Knappe, MEMS atomic clocks, Compr. Microsyst. 3 (2007) 571–612.
[9] Y. Pétremand, C. Affolderbach, R. Straessle, et al., Microfabricated rubidium vapour cell with a thick glass core for small-scale atomic clock applications, J. Micromech. Microeng. 22 (2012) 025013.
[10] D. Miletic, C. Affolderbach, E. Breschi, et al., Fabrication and spectroscopy of Cs vapour cells with buffer gas for miniature atomic clock, EFTF-2010 24th European Frequency and Time Forum, IEEE, 2010.
[11] V.V. Zabrodsky, V.P. Belik, P.N. Aruev, et al., A study of vacuum-ultraviolet stability of silicon photodiodes, Tech. Phys. Lett. 38 (9) (2012) 812–815.
[12] A.P. Artyomov, S.A.E.Kh. Baksht, V.F. Tarasenko, et al., Vremennye kharakteristiki kremnievykh detektorov vakuumnogo ul'trafioletovogo i myagkogo rentgenovskogo izlucheniya (Temporal characteristics of silicon detectors of vacuum ultraviolet and soft X-rays), ПТЭ 1 (2015) 104–108.
[13] A.B. Post, Y.-Y. Jau, N.N. Kuzma, et al., End resonances for atomic clock, in: Proceedings of 35th Annual Precise Time and Time Interval (PTTI) Systems and Applications Meeting, Long Beach, California, USA, 2003, pp. 445–455.
[14] J. Kitching, S. Knappe, L. Hollberg, Miniature vapor-cell atomic-frequency references, Appl. Phys. Lett. 81 (2002) 553–555.

[15] A.A. Baranov, S.V. Ermak, V.V. Semenov, Orientational frequency shifts of microwave 0–0 superfine resonance in ^{87}Rb vapor with selective optical pumping, Opt. Spectrosc. 114 (3) (2013) 337–339.

[16] V.V. Semenov, P.V. Zimnitskii, R.V. Smolin, S.V. Ermak, The effect of flicker processed on the resolution of self-oscillating magnetometers optically pumped in the saturation regime, Tech. Phys. Lett. 40 (3) (2014) 271–273.

[17] A.A. Baranov, S.V. Ermak, V.V. Semenov, Orientation light shift suppression in alkali atom microwave standards with laser pumping, Proc. EFTF Art. no. 6502336 (2012) 72–73.

[18] A.A. Baranov, S.V. Ermak, V.V. Semenov, The orientation dependence of the SHF radio–optical resonance frequency light shift in rubidium vapors, Proc. IEEE IFCS Art. no. 5977289 (2011).